Gadolinium silicide (Gd₅Si₄) nanoparticles for tuneable broad band microwave absorption

Pritom J. Bora, ¹ S. M. Harstad, ² S. Gupta, ³ V. K. Pecharsky, ^{3,4} K. J. Vinoy, ⁵ Praveen C. Ramamurthy* ^{1,6} and R. L. Hadimani * ^{2,7}

Dept. of Electrical and Computer Engineering, Iowa State University, USA

* Corresponding authors:

Praveen C. Ramamurthy: onegroupb203@gmail.com

Ravi L. Hadimani: rhadimani@vcu.edu

¹ Interdisciplinary Centre for Energy Research (ICER), Indian Institute of Science, India.

² Department of Mechanical and Nuclear Engineering, Virginia Commonwealth University, USA.

³ Ames Laboratory, Division of Materials Science and Engineering, U.S. Department of Energy, USA

⁴ Department of Materials Science and Engineering, Iowa State University, USA.

⁵ Department of Electrical and Communication Engineering, Indian Institute of Science, India.

⁶ Department of Materials Engineering, Indian Institute of Science, India.

Abstract

Soft magnetic Gd₅Si₄ nanoparticles exhibit excellent microwave absorption in the Ku-band (12.4-18 GHz) when dispersed in poly (dimethyl siloxane), PDMS. The minimum experimentally recorded reflection loss (RL) of Gd₅Si₄-PDMS nanocomposite is -69 dB, with a large bandwidth for a single 6 mm-thick layer. The bandwidth can be further extended by using a novel design where 1 mm-thick layers of the nanocomposite are arranged into a modified pyramid-shaped absorber. Standard electromagnetic (EM) simulations confirm experimental results.

1. Introduction

Interest in microwave absorbing materials, especially those suitable for high frequency (Ku-band, 12.4-18 GHz) absorption, is on the rise due to a rapid progress in radar and military aircraft [1-5]. A number of magnetic materials have been proposed for microwave absorption due to specific advantages, including impedance matching [2-6]. Ferrite based materials such as nickel-zinc ferrite, and cobalt-zinc ferrite are well known, readily available microwave absorbers [7-9]. Engineered nano-structures and nano-composites have also been suggested as useful materials for enhanced absorption [10, 11]. Hybrid conducting polymer–magnetite nanocomposites such as polyaniline (PANI)-Fe₂O₃, PANI-NiFe₂O₄, PANI-CoFe₂O₄ nanocomposites demonstrate high microwave absorption properties and may be useful for shielding applications [12-14], however, stability of a conducting polymer(s) is the challenge [15]. On the other hand, polymer nanocomposites have numerous advantages, such as being lightweight, flexible, corrosion resistant, and inexpensive [16, 17]. Effect of nano-filler and micro-filler ferrites for microwave absorption in polymer matrix was reported in the literature [18]. Nano-fillers are shown to be suitable for high frequency (> 6 GHz) absorption, whereas micro-filler ferrites show better absorption in low frequency region (< 6 GHz) [18-22]. Soft magnetic materials are also advantageous for broad band microwave absorption [23].

Despite a number of useful compounds, new materials suitable for microwave absorption are always a key interest [24, 25]. Soft ferromagnetic gadolinium silicide (Gd₅Si₄) nanoparticles are novel materials exhibiting a range of properties potentially useful for various applications [26-28]. While the magnetic properties of Gd₅Si₄ nanoparticles have been reported [29] their microwave absorption performance have not been examined. In this work we investigate the microwave absorption properties of a nanocomposite containing Gd₅Si₄ nanoparticles and standard flexible poly (dimethyl siloxane) (PDMS) rubber.

2. Experimental

Nanoparticles of Gd₅Si₄ were prepared by first grinding as-cast bulk stoichiometric alloy, synthesized by arc-melting, into a powder with particle sizes below 45 μm. Further size reduction was carried out using high-energy ball-milling with addition of 10 wt.% poly(ethylene glycol) (PEG) as a surfactant. The milling itself was carried out in two steps, in which the Gd₅Si₄ powder/PEG mixture was first milled for 1 h, after which 5 ml of heptane were added to the vial and milling was continued for another hour. Further details about the particle preparation process can be found in Refs [26-29]. To study the dielectric and microwave absorption properties of Gd₅Si₄, optimally, 40 wt.% of as synthesized Gd₅Si₄ was mixed with PDMS, and then poured into a rectangular copper sample holder (Ku-band). The mixture was dried in a vacuum oven at 60±3 °C for 6 h. The obtained composite henceforth is referred to as PGS.

The cross-sectional and surface morphology, energy dispersive X-ray (EDX) studies of PGS were carried out in a field emission scanning electron microscope (FESEM, Carl Zeiss). The dielectric properties of both the PDMS and the prepared PGS nanocomposite were measured in the Ku-band (12.4-18 GHz) by using Agilent vector network analyser (Agilent N5201). The thru-reflect-line (TRL) calibration is the standard calibration method (also industrial standard) to obtain the complex S-parameters (S_{II} , S_{I2} , S_{2I} , S_{22}) [30]. A complete two port TRL calibration was performed in the Ku-band, before commencement of the measurements. Using the obtained S-parameters, relative permittivity ($\varepsilon_r = \varepsilon' - i\varepsilon''$) and permeability ($\mu_r = \mu' - i\mu''$) values were determined using the standard Nicholsion-Ross-Weir (NRW) algorithm [30]. The reflection loss (RL) of a single-layer metal-backed absorber was calculated using the following standard equation [31, 32],

$$RL(dB) = 20log \left| \frac{Z_{in} - Z_0}{Z_{in} + Z_0} \right|, \tag{1}$$

where, Z_0 (=377) and Z_{in} correspond to the free space intrinsic impedance and the composite material impedance, respectively. Z_{in} is given by,

$$Z_{in} = Z_0 \sqrt{\frac{\mu_r}{\varepsilon_r}} \tanh\left(j \frac{2\pi f d\sqrt{\mu_r \varepsilon_r}}{c}\right),\tag{2}$$

where, f is the frequency, d is the thickness of the absorbing material and c is the velocity of light (3×10⁸ ms⁻¹).

3. Results and discussion

Surface morphology of as synthesized Gd₅Si₄ nanoparticles with low and high magnifications, respectively, is shown in **Fig. 1(a)** and **Fig. 1(b)**. The SEM images reveal irregularly shaped nanoparticles with certain size distribution. The advantage of irregularly shaped nanoparticles over spherical is higher surface area and resulting easy formation of linkages in the polymer matrix, achieving percolation threshold at lower particle loading. The X-ray diffraction pattern of Gd₅Si₄ nanoparticles is as shown in **Fig. 1(c)**, indicating that the major phase is Gd₅Si₄ and the minor phase is Gd₅Si₃. The vibrating sample magnetometry (VSM) measurements illustrated in **Fig. 1(d)** confirm soft magnetic behaviour of Gd₅Si₄ nanoparticles at room temperature.

The cross sectional surface morphology of PGS and corresponding EDX results are depicted in **Fig. 2**. As expected, the EDX results suggest that the major element in PGS is Gd. The cross sectional surface morphology of PGS points to a satisfactory linkage of Gd₅Si₄ in PDMS.

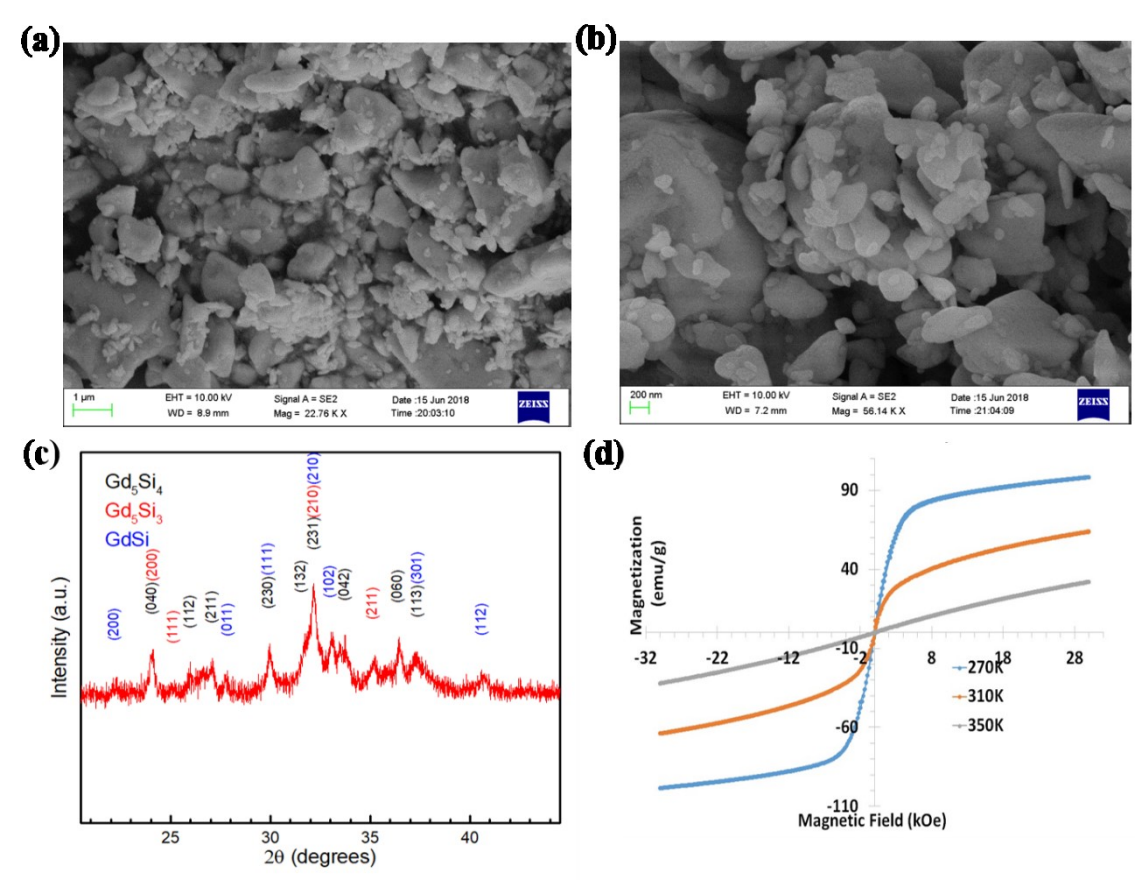


Fig.1. Surface morphology with **(a)** low and **(b)** high magnifications, **(c)** X-ray powder diffraction pattern, and **(d)** room temperature hysteresis loops of Gd₅Si₄ nanoparticles.

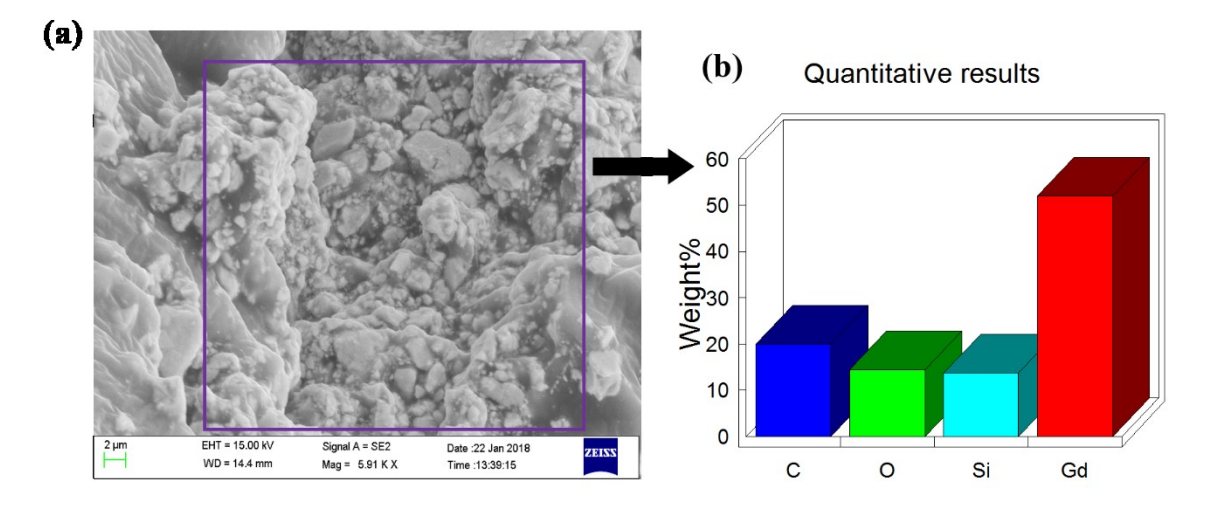


Fig.2. (a) Cross sectional surface morphology of PGS and (b) corresponding EDX result.

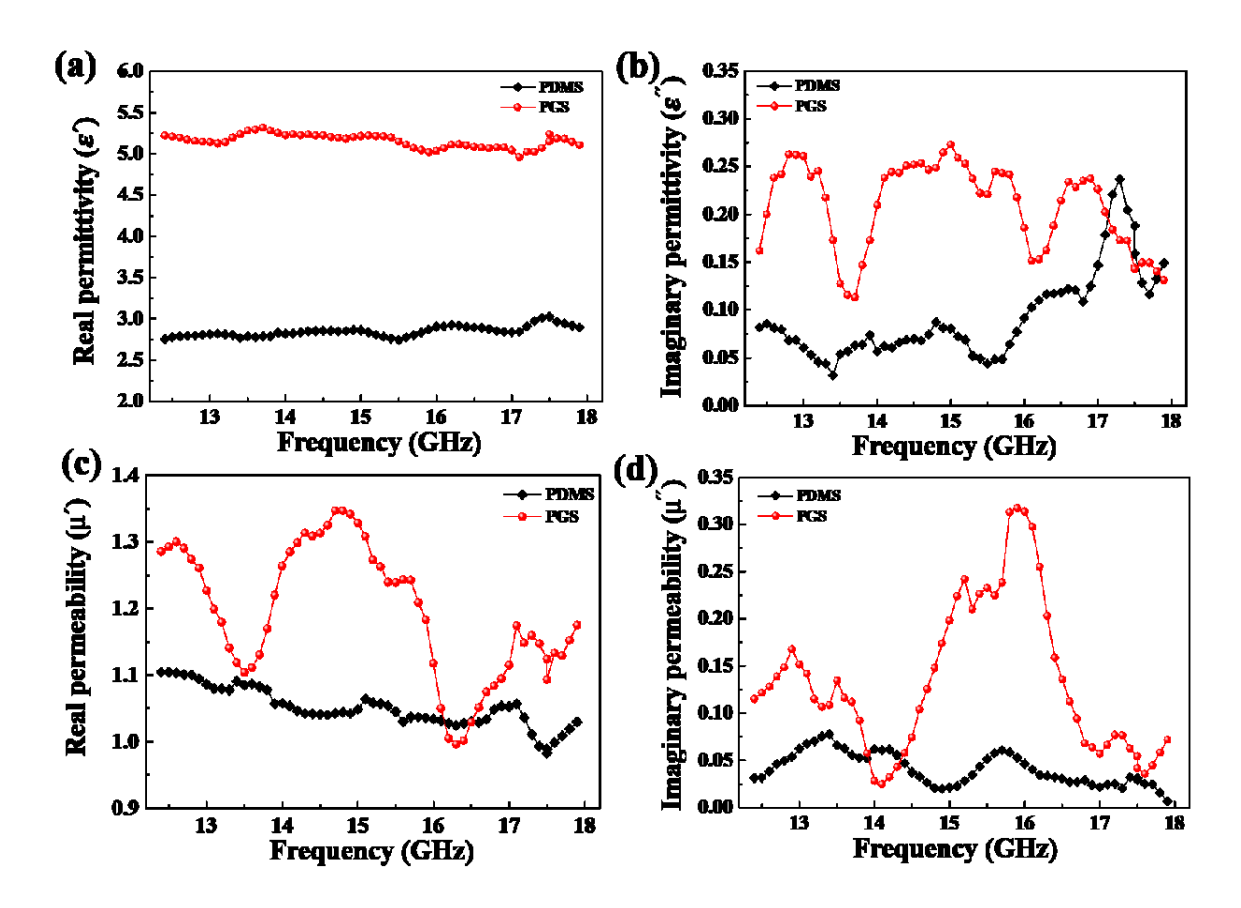


Fig. 3. Variation of (a) real (ϵ') and (b) imaginary (ϵ'') parts of complex electric permittivity, and (c) real (μ') and (d) imaginary (μ'') parts of complex magnetic permeability of PGS and PDMS in the Kuband (12.4-18 GHz).

The variation of the real (ϵ') and imaginary (ϵ'') parts of complex electric permittivity of PGS and PDMS in the Ku-band (12.4-18 GHz) is shown in **Fig. 3(a)** and **Fig. 3(b)**, respectively. The first represents the ability of a material to store electric energy and is related to the amount of polarization, whereas the second corresponds to the electric energy dissipation inside the material. Similarly, the real and imaginary parts of complex magnetic permeability (μ' and μ'') represent, respectively, the magnetic energy storage capacity and the dissipation of magnetic energy. The ϵ' values of Gd₅Si₄-loaded PDMS (PGS) are between ~5 and 5.5, and ϵ'' varies between ~ 0.10 and 0.25 in the Ku-band, compared to ϵ' and ϵ'' of ~2.5 and ~0.05, respectively, of PDMS alone. A minor but noticeable reduction of ϵ'' of PGS with frequency is believed to be due to the interfacial polarization between PDMS and Gd₅Si₄ as well as

synergistic effect of the matrix and filler. The variation of permittivity and multiple resonance behaviour are associated with electron polarization, ion polarization, space charge polarization, dipole polarization and interfacial polarization [21, 9]. However, the ion and electron polarization is more prominent in the THz range [21], therefore, the observed resonance of permittivity of PGS originates from the space charge polarization, dipole polarization and interfacial polarization. The change in ε'' values ($\Delta \varepsilon''$) indicate that interfacial polarization is the major factor in this nanocomposite [33]. The variation of μ' and μ'' values of PGS and PDMS are both shown in Fig. 3(c) and Fig. 3(d). Due to the soft ferromagnetism of Gd₅Si₄, μ' and μ'' of PGS vary significantly between 12.4 and 18 GHz. The variation of μ' (between ~1.35 and 1) can be attributed to the Snoek's limitation in the GHz range [23]. Similarly, multiple peaks in μ" for PGS (the highest peak viz. 0.32) may be due to the natural resonance and exchange resonance [9, 21, 23]. In general, the strong fluctuations of μ' and μ'' values was observed due to the hysteresis loss, domain wall resonance, natural resonance and exchange resonance as well as eddy current effect [23]. However, domain wall resonance is predominant for 1-100 MHz and hysteresis loss can be ignored for a weak applied field [21, 23]. According to the ferromagnetic resonance theory, the natural resonance frequency (f_r) and the anisotropy energy (H_a) can be expressed as [9],

$$f_r = \gamma \frac{H_a}{2\pi} \tag{3}$$

Where, γ is the gyromagnetic ratio. The H_a value depends on saturation magnetization (M_s) and it is also related to the anisotropic constant [9]. Therefore, it may be suggested that, in case of PGS, the natural resonance is predominant along with exchange resonance.

The thickness-dependent reflection loss (RL) of PGS is shown in **Fig. 4(a)** and **Fig. 4(b)**. For practical applications RL of -10 dB, which corresponds to a 90 % absorption, is believed to be an adequate level [31, 32]. In the case of PGS, a minimum RL value of -23 dB

was recorded at 2 mm thickness with a 2.1 GHz bandwidth, f_E , where RL remains lower than -10 dB in the Ku-band, as illustrated in **Fig. 5 (a)**. When thickness increases, the minimum RL decreases and the bandwidth expands, -69 dB and 3.3 GHz, respectively, at 6 mm thickness as illustrated in **Fig. 5 (b)**. Interestingly, RL is near minimum in the middle of the Ku-band region (13-17 GHz) for this thickness. The variation of RL with respect to frequency for different thicknesses can be understood through the quarter-wavelength equation which is related to the matching thickness (d_m) and wavelength (λ), ^{34, 35}

$$d_m = \frac{n\lambda}{4} \tag{4}$$

Here, n = 1, 3, 5...

$$\lambda = \frac{c}{f\sqrt{|\varepsilon_r|\,|\mu_r|}}\tag{5}$$

When absorption corresponding frequency and thickness obeys the above criteria, the two reflected waves, viz., air-absorber interference and absorber-perfect electric conductor (PEC) interface are out of phase by 180°, leading to disappearance of them on the absorber resulting minimum RL value. Hence, minimum RL value was obtained for a specific frequency for a given absorber thickness and inversely related to frequency.

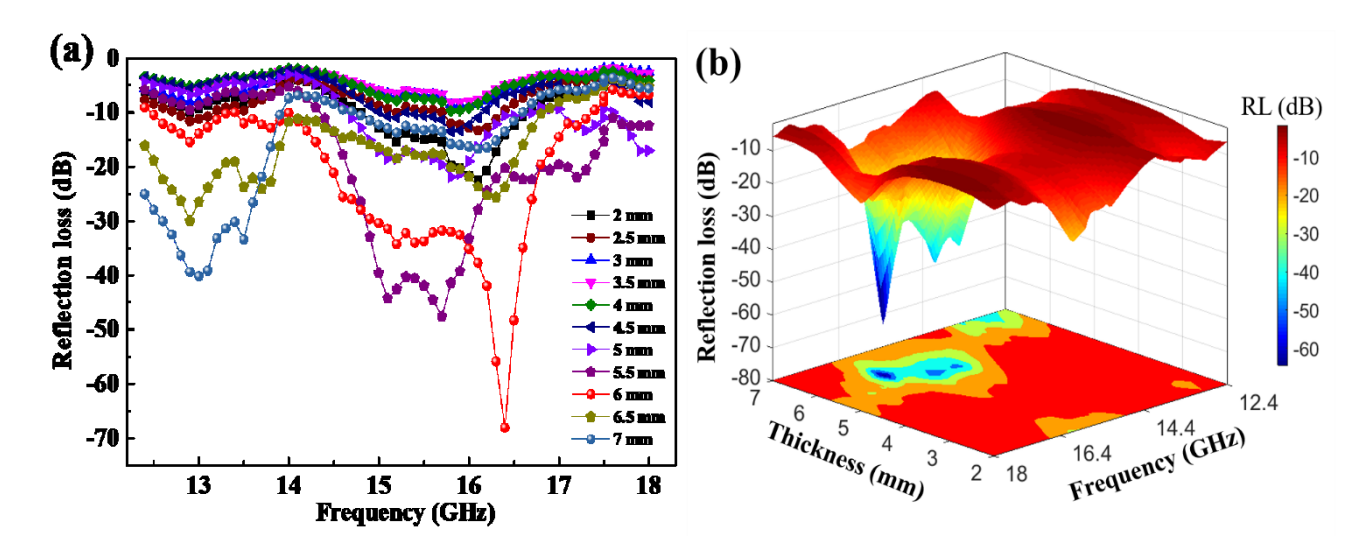


Fig. 4. (a) Ku-band reflection loss (RL) of PGS at various thickness and (b) 3D representation of RL (dB) values for PGS.

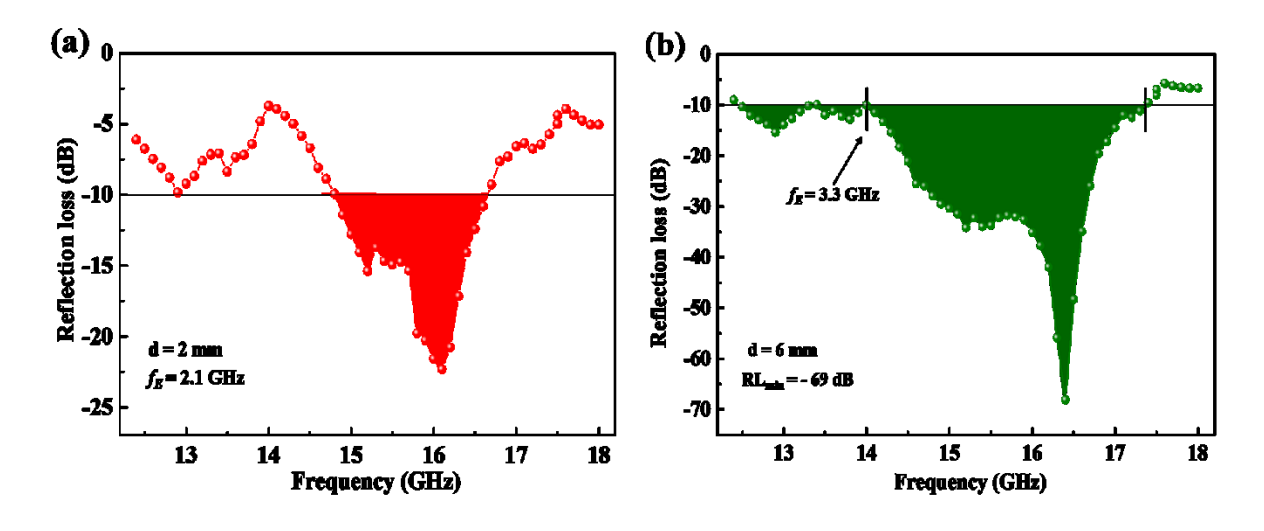


Fig. 5. Ku-band reflection loss (RL) of PGS at (a) 2 mm and (b) 6 mm thickness.

The minimum RL value obtained for PDMS was -6 dB at 6 mm thickness. Fig. 6 (a) and Fig.6(b) shows that PDMS is a much weaker microwave absorber compared to PGS. In fact, the optimal RL of -10 dB is not possible even at 6 mm thickness. This is in stark contrast to the minimum RL of -69 dB with a large bandwidth demonstrated for a 6 mm thick layer of PGS. Clearly, the strong enhancement of microwave absorption in PGS compared to PDMS is due Gd₅Si₄ nanoparticles embedded in the former. The RL value for different loading of Gd₅Si₄ nanoparticles in PDMS were given in the *supporting information* (Fig. S2). A comparison with some recently reported hybrid microwave absorber at high frequencies.

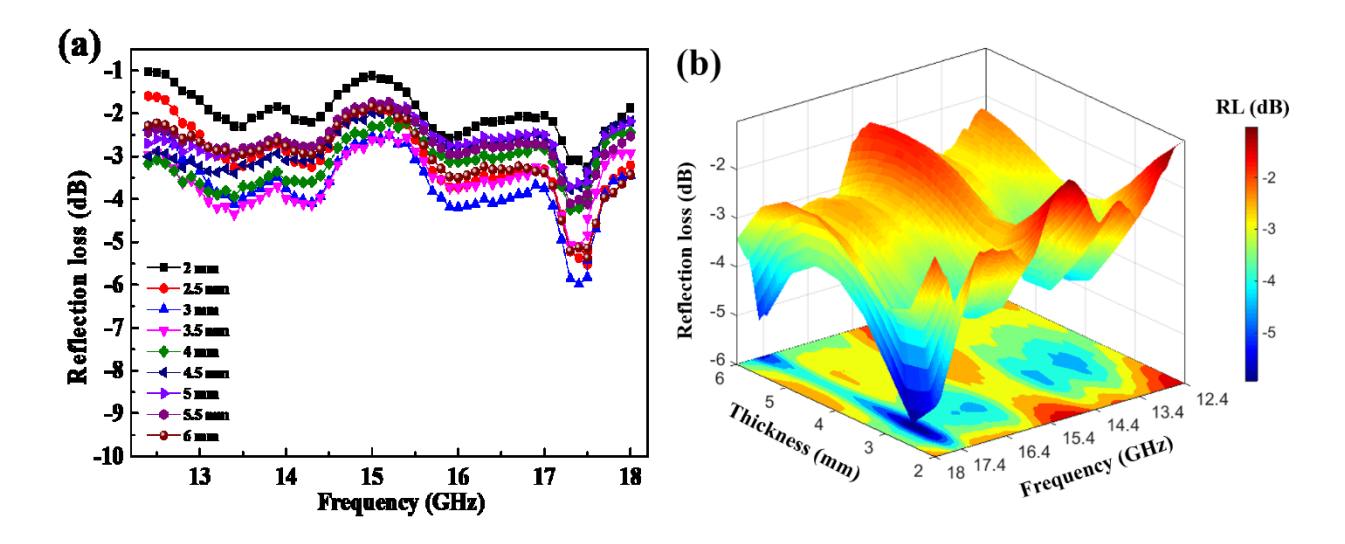


Fig.6. (a) Ku-band reflection loss (RL) of PDMS at various thickness and (b) 3D representation of RL (dB) values for PDMS.

Table.1. Reflection loss (RL in dB) of selected magnetic hybrid materials.

No	Material	Filler	Minimum RL	Frequency range	Thickness	Reff
		Wt %/	(dB)	(GHz)	(mm)	
		Ratio		$(RL \le -10 dB)$		
1	Paraffin/Fe nanoflakes	40 %	-9	~ 9	2	36
2	Paraffin / Fe-SiO ₂	40 %	-15	7-15	2	36
3	Epoxy/γ-Fe ₂ O ₃	80 %	-15	10.2-10.5	3	37
4	Epoxy/Fe ₂ O ₃ nanoflower	80 %	-15	10-14	2	37
5	Epoxy / Fe-CMK3	31.8 %	-18	11-12.4	1.6	38
6	Paraffin / MnO ₂ -Fe	1:1	-16	11-13	3	39
7	Epoxy / Fe micron fibre	20%	-11	7-7.5	1.5	40
8	Paraffin/graphene@SiO2	25%	-12.5	16-18	2	41
	@NiO nanoflowers					
9	Paraffin wax/ CoO	70%	-12.3	13-15	3	42
	nanobelts					
10	Epoxy/ NiFe ₂ O ₄	2:1	-12.5	~ 2.5	2	13
11	Epoxy/polyanilie-	2:1	-20.3	3-5	2	13
	$NiFe_2O_4$					
12	$Paraffin \ / Co_{0.6} Zn_{0.4} Fe_2 O_4$	20 %	-17	5.8-11.5	3.6	8
			-22	14-16	7	
13	Paraffin wax/RGO-Fe ₃ O ₄	40 %	-20	5.5-7	3.5	43
14	Silicon rubber/	70 %	-20	5-7	5.5	7
	$Ni_{0.5}Zn_{0.5}Fe_2O_4$					
15	PDMS- Gd_5Si_4	40 %	-23	14.5-16.6	2	This
			-69	12.4-17.5	6	Work

The mechanism behind the excellent microwave absorption properties of PGS can be understood considering dielectric loss tangent $(tan \, \delta_e)$, magnetic loss tangent $(tan \, \delta_m)$, impedance matching, as well as from electro-magnetic (EM) attenuation coefficient (α) [1-9]. The loss tangents, calculated as

$$\tan \delta_e = \frac{\varepsilon''}{\varepsilon'}$$

$$\tan \delta_m = \frac{\mu''}{\mu'}$$

are shown in Fig. 7. The dielectric loss tangent of PGS, $tan \delta_e \cong 0.05$, is somewhat larger, than the same (~0.03) for PDMS. The magnetic loss tangents are, however, significantly different, especially in the middle of the Ku-band. The peak value $tan \delta_m = 0.28$ of PGS is much higher when compared to common magnetic-composite absorbers, clearly suggesting that the magnetic loss is the key factor in achieving promising RL. The magnetic loss occurs due to eddy currents, and natural and exchange resonance in the electromagnetic wave frequency band, and the eddy current effects must be suppressed in order for a material to serve as a good microwave absorber [31]. If magnetic losses are solely due to eddy current, the factor, $C_0 = \mu''(\mu')^{-2} f^{-1} = 2\pi\mu_0 \sigma s^2/3$ (where σ is the electric conductivity and s is the particle diameter) should remain frequency-independent [31, 32]. As shown in Fig. 8, C_0 of PGS varies by an order of magnitude, hence, the effect of eddy currents on the magnetic loss here may be ignored. Further, the synergetic effect between dielectric loss and magnetic loss in PGS nanocomposite also makes a contribution towards broadband microwave dissipation and hence absorption.

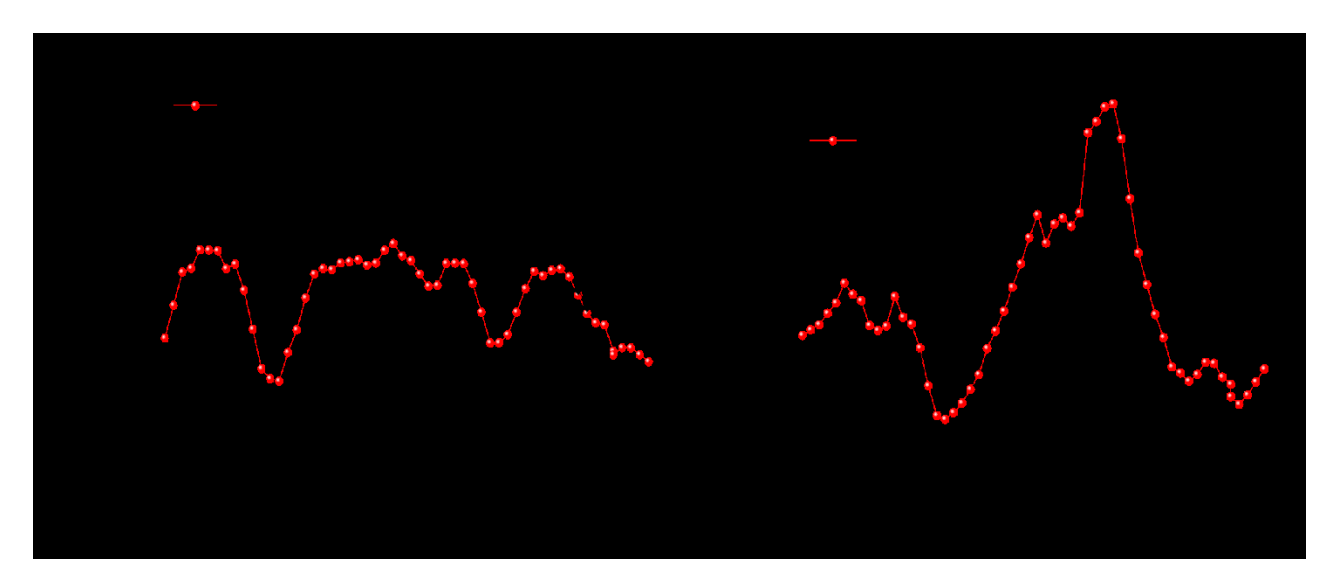


Fig.7. (a) Dielectric $(\tan \delta_e)$ and (b) magnetic $(\tan \delta_m)$ loss tangent of PGS and PDMS in the Kuband.

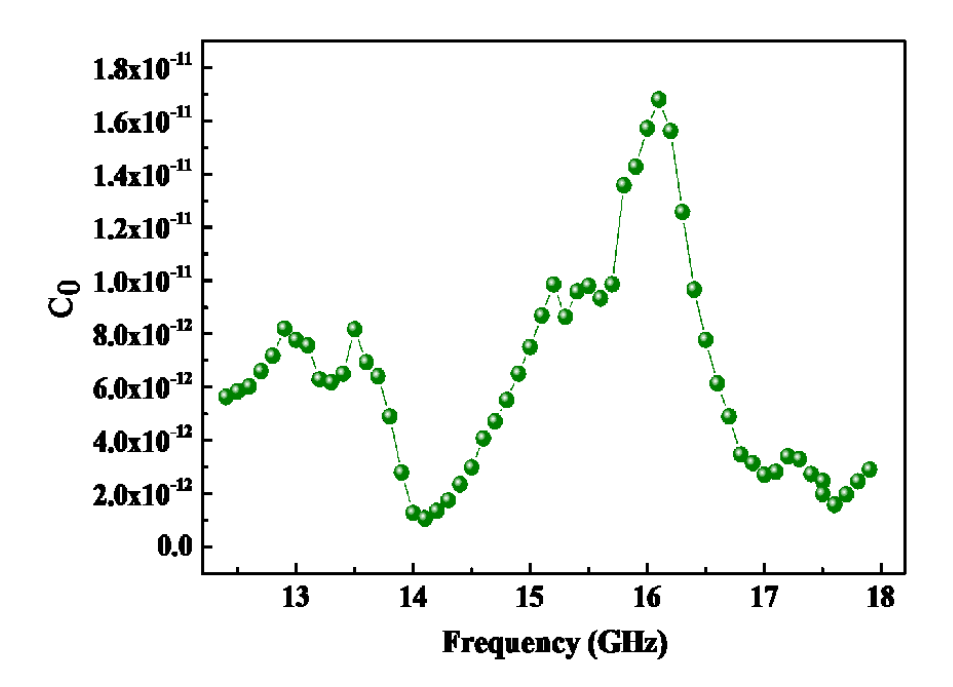


Fig.8. Variation of C_0 of PGS in the Ku-band.

According to the transmission line theory, EM attenuation coefficient (α) is given by [31-35],

EM attenuation coefficient (α)

$$= \frac{\sqrt{2}\pi f}{c} \times \left[\left(\mu^{"} \varepsilon^{"} - \mu' \varepsilon' \right) + \left\{ \left(\mu^{"} \varepsilon^{"} - \mu' \varepsilon' \right)^{2} + \left(\mu' \varepsilon^{"} + \mu^{"} \varepsilon' \right)^{2} \right\}^{\frac{1}{2}} \right]^{\frac{1}{2}}$$
(8)

In the Ku-band, EM attenuation coefficient of PDMS varies weakly between 13 and 30 (**Fig. 9**), whereas the same for PGS, especially in the middle of the frequency range (14-17 GHZ), varies stronger and reaches much higher values of 24-125. This indicates the excellent EM attenuation power of PGS especially in this frequency region.

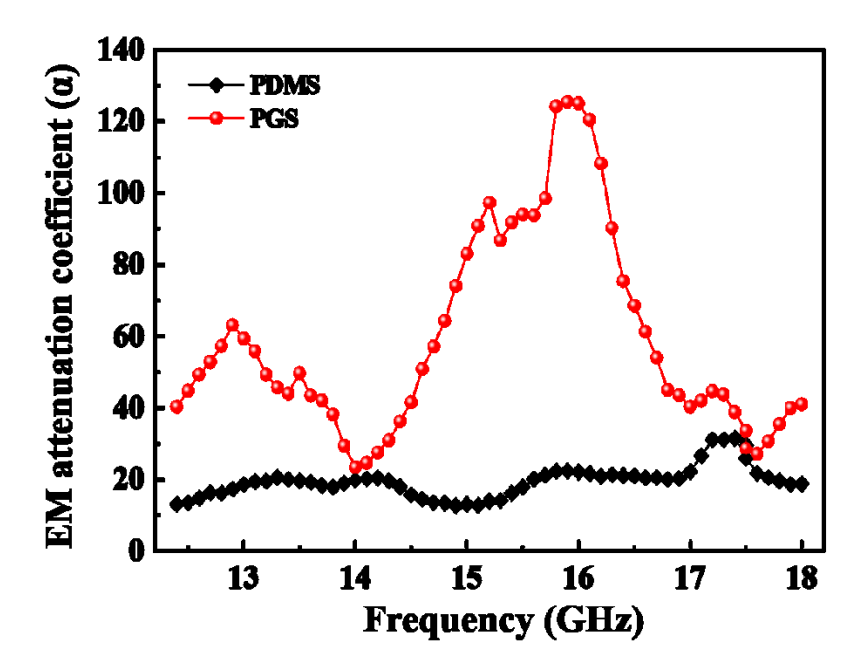


Fig.9. Calculated EM attenuation coefficients of PDMS and PGS in the Ku-band.

For an ideal microwave absorber, the impedance matching condition of the absorption material and free space is the prerequisite condition [11]. For that both permittivity and permeability value should be same or similar [11]. The impedance matching degree (Δ) can be expressed as [11],

$$\Delta = |\sinh^2(Kfd) - M| \tag{9}$$

Where, *K* and *M* is given by,

$$K = \frac{4\pi\sqrt{\mu'\epsilon''}}{c} \frac{\sin[(\delta_e + \delta_m)/2]}{\cos\delta_e \cos\delta_m} \tag{10}$$

$$M = \left[4\mu'\cos\delta_{e}\varepsilon'\cos\delta_{m}\right].\left[\left(\mu'\cos\delta_{e} - \varepsilon'\cos\delta_{m}\right)^{2} + \left(\tan\frac{\delta_{m}-\delta_{e}}{2}\right)^{2} \left(\mu'\cos\delta_{e} + \varepsilon'\cos\delta_{m}\right)^{2}\right]^{-1}$$
(11)

Notably, for a strong microwave absorption material, Δ value should be minimum [11]. Since permittivity and permeability both are predominant in PGS, therefore expected Δ value

is also minimum, indicates the better impedance match condition between the PGS and free space. In addition to the above discussion, the irregular shaped Gd₅Si₄ nanoparticles induces multiple reflections and scattering of incident microwave and prolong the travel pathway in the PGS to attenuate microwave energy [21]. Under the influence of an alternating electromagnetic field, the charge accumulation between the Gd₅Si₄ and PDMS matrix takes place through the numerous micro capacitors formed due to the PDMS dielectric in between two Gd₅Si₄ nanoparticles, as explained in the literature [21]. These micro capacitors are also helping to strong microwave absorption of PGS through leakage current loss and associated polarizations [21].

To determine the power distribution, a standard EM simulation was carried out using CST-microwave studio. The schematic of the absorber (PGS) structure is shown in Fig. 10(a) and Fig. 10(b) respectively. As a case study, 0.5 W stimulation was assumed at the source port, and the power absorbed, reflected and lost in PEC (metal) for PGS and PDMS absorbing structures are, respectively, shown in Fig. 11 and Fig. 12. As shown in Fig.11, the stimulated power is predominantly absorbed (more than 90%) by a 6 mm layer of PGS. No loss in the conducting surface (PEC or metal) was observed. On the other hand, the absorbed power is much smaller for PDMS (~10 %, Fig. 12) indicating the excellent microwave power absorption property of Gd₅Si₄ nanoparticles in polymer (PDMS). The dissipation of power density inside the PGS (6 mm) at the constant 16.4 GHz frequency is as shown in Fig. S1 (Supporting information).

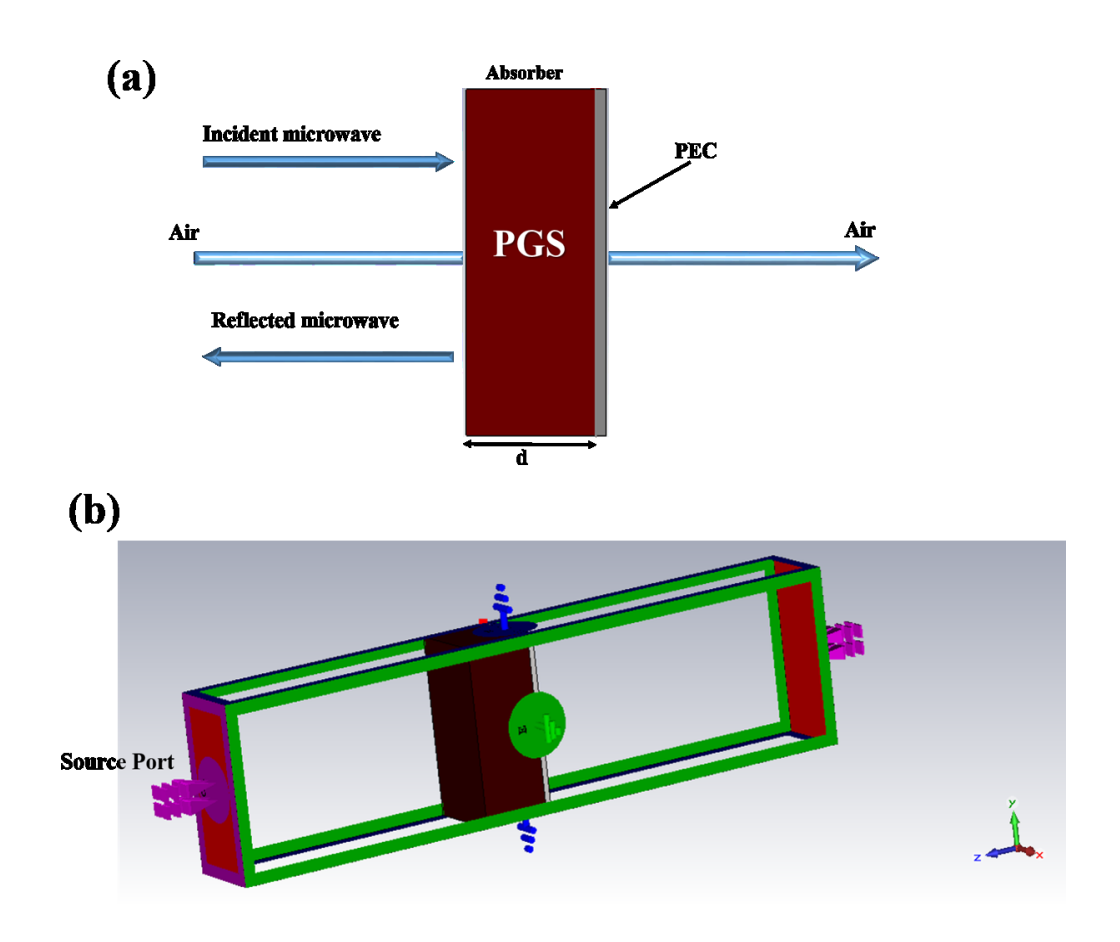


Fig. 10. Schematic of (a) PGS absorbing structure and (b) typical waveguide measurement.

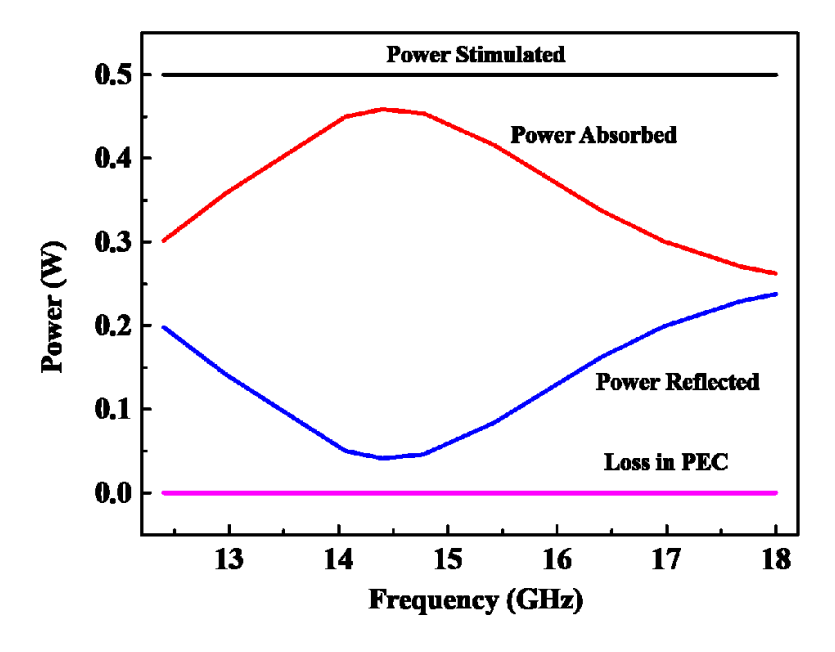


Fig. 11. Power stimulated, absorbed, reflected and lost in a conducting surface (PEC) for a 6 mm layer of PGS.

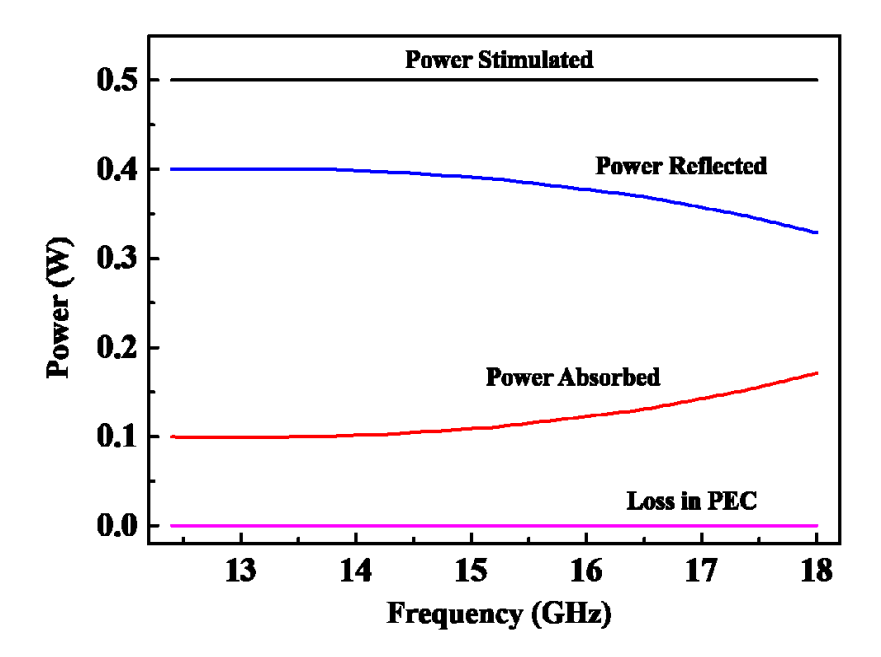


Fig. 12. Power stimulated, absorbed, reflected and lost in a conducting surface (PEC) for a 6 mm PDMS.

The loss factor (LF), given by [45],

Loss Factor (%) =
$$100 \times (1 - |S_{11}|^2 - |S_{21}|^2)$$
 (12)

is shown in **Fig. 13** for various thicknesses of PGS. The maximum LF values (more than 90 %) in the Ku-band are observed at 5-7 mm, which appears to be the most effective range for microwave absorption, but even at 2 mm, loss factor remains fairly high, exceeding 50 %. When the thickness is increased from 5 mm to 7 mm, the maximum LF values shift to low frequency region, which is related to the quarter wavelength matching (*Eqn. 3*).

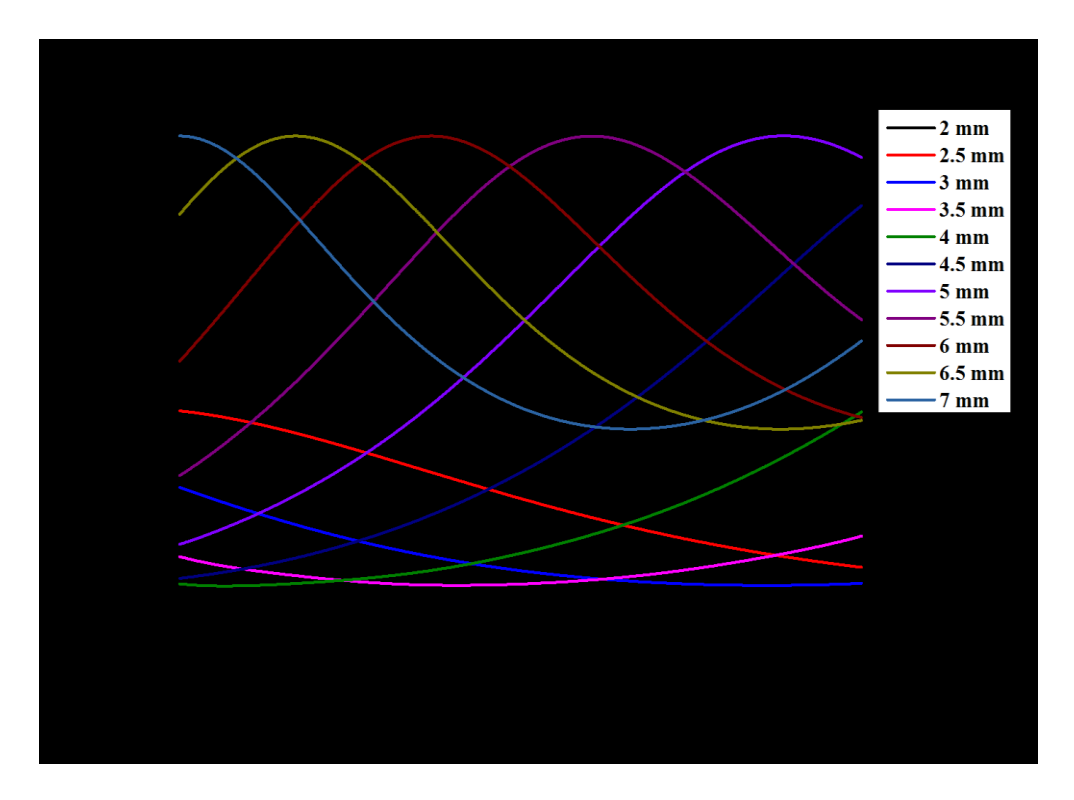


Fig.13. Simulated loss factor of PGS at various thickness in the Ku-band.

In practice, tunability of the microwave absorption bandwidth is tremendously important, although it is well known that achieving a large bandwidth with a single layer is difficult [46]. Among possible solutions, various absorbing structures can be employed, including a recently proposed modification of a conventional pyramidal microwave absorbing architecture [46]. Based on that, an artificial array of the designed pyramids and the unit cell (pyramid) of PGS nanocomposite are shown in **Fig. 14(a)** and **Fig. 14(b)**, respectively. Here, the 6 mm PGS with 10×10 mm² area was divided into 6 layers of 1 mm each (**Fig. 14(b)**), and the excitation port was introduced at *z* max so that EM wave propagates along the Z-axis, i.e., along the layer stacking direction. For tuning the unit cell size, a magnified parameter "m" was assigned and swept from m =1 mm to m = 1.6 mm. The resulting RL is shown in **Fig. 15**.

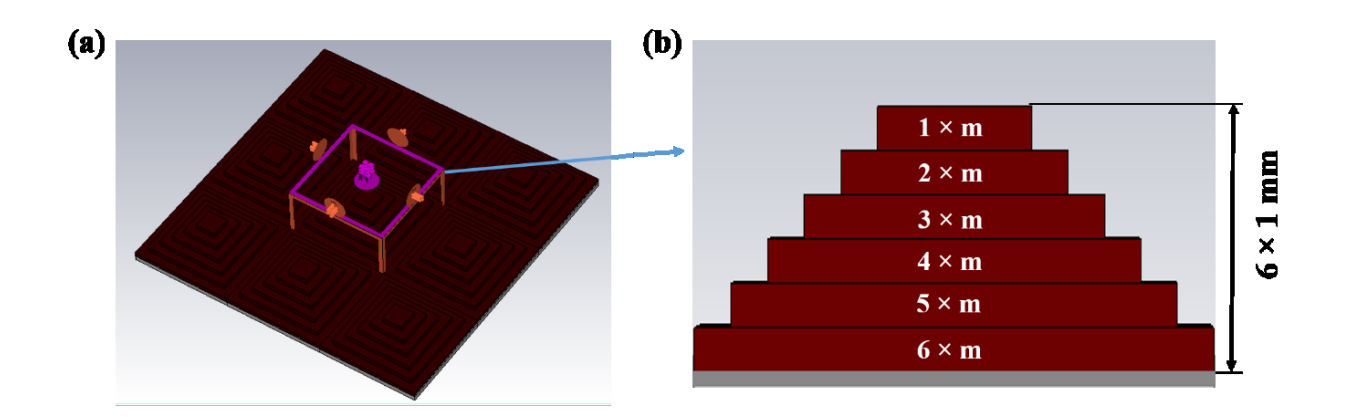


Fig.14. (a) Designed artificial multilayer periodic pattern of PGS, (b) schematic of a unit cell.

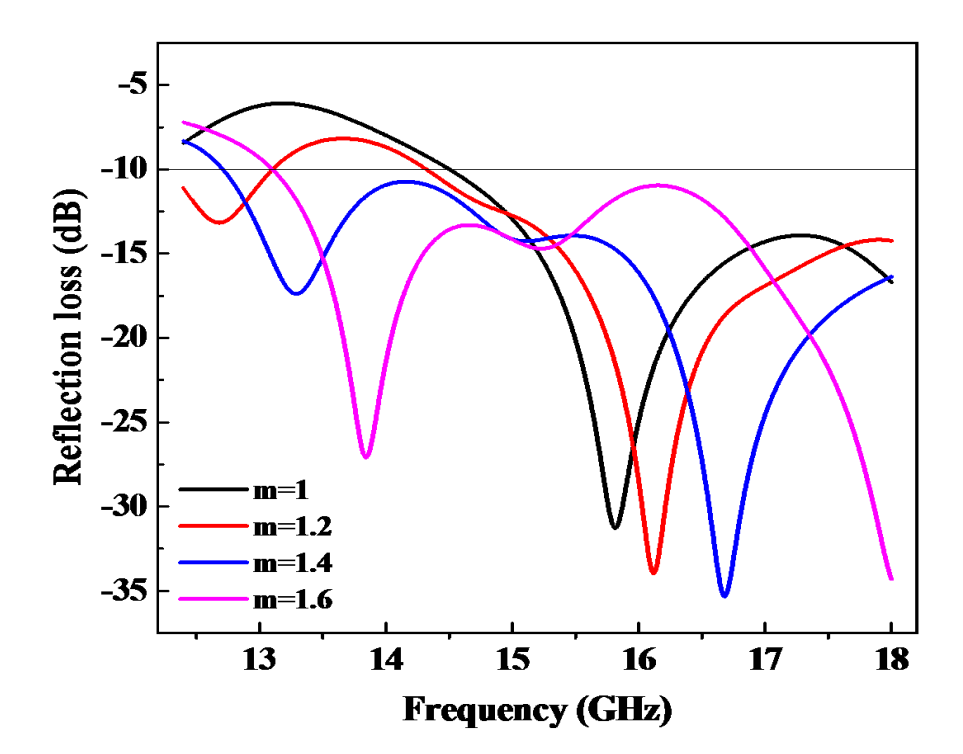


Fig.15. Simulated microwave absorption performance of designed artificial multilayer periodic pattern of PGS.

Simulated results shown in **Fig. 15** indicate that, for the total thickness of 6 mm, a large absorption bandwidth of PGS nanocomposite can be tuned with the proposed pyramidal design. In the case of single layer PGS (6 mm), the highest bandwidth was 3.3 GHz (12.4-17.5 GHz). For m =1.4 mm, the obtained bandwidth was increased to 5.35 GHz. Further, as shown in **Fig. 15**, a large bandwidth can be tuned by changing m value.

4. Conclusions

The microwave absorption properties of Gd₅Si₄ nanoparticle-polymer composite is promising. A minimum RL value of -69 dB was achieved in the middle of Ku-band with bandwidth for a single layer PGS (6 mm) reaching 3.3 GHz (14-17.3 GHz). However, when thickness decreases to 2 mm, the bandwidth also decreases to 2.1 GHz (14.6-16.7 GHz). Microwave absorption bandwidth of the nanocomposite can be further enhanced using an array of pyramidal microwave absorbing architecture. The magnetic loss tangent of the composite was found to be higher than the dielectric loss tangent, indicating that in this material eddy current effects can be ignored. EM simulations also show that compared to pure PDMS, the absorption power of the same at 40% loading with Gd₅Si₄ nanoparticles is much higher. The latter, therefore, may be suggested as a potential candidate for microwave absorption applications in the Ku-band.

Acknowledgments

PJB and PCR gratefully acknowledge the technical support from MNCF (CeNSE), IISc for this work. SG and VKP acknowledge support by the Division of Materials Science and Engineering of the Office of Basic Energy Sciences of the U.S. Department of Energy.

Preparation and characterization of Gd₅Si₄ in bulk and nanoparticulate forms was performed at Ames Laboratory, which is operated for the U.S. Department of Energy by Iowa State University of Science and Technology under Contract No. DE-AC02-07CH11358.

Work at VCU is partly supported by National Science Foundation, Award Numbers: 1610967 and 1726617.

References

- [1] X. G. Liu, B. Li, D. Y. Geng, W. B. Cui, F. Yang, Z. G. Xie, D. J. Kang and Z. D. Zhang, *Carbon N. Y.*, 2009, **47**, 470–474.
- [2] F. Qin and H. X. Peng, *Prog. Mater. Sci.*, 2013, **58**, 183–259.
- [3] P. J. Bora, M. Porwal, K. J. Vinoy, Kishore, P. C. Ramamurthy and G. Madras, *Compos. Part B Eng.*, 2018, **134**, 151–163.
- [4] K. J. Vinoy and R. M. Jha, Sadhana, 1995, 20, 815–850.
- [5] B. Zhao, X. Guo, Y. Zhou, T. Su, C. Ma and R. Zhang, *CrystEngComm*, 2017, **19**, 2178–2186.
- [6] P. J. Bora, M. Porwal, K. J. Vinoy, P. C. Ramamurthy and G. Madras, *Mater. Res. Express*, DOI:10.1088/2053-1591/3/9/095003.
- [7] Y. Hwang, *Mater. Lett.*, 2006, **60**, 3277–3280.
- [8] L. Yan, J. Wang, Y. Ye, Z. Hao, Q. Liu and F. Li, J. Alloys Compd., 2009, 487, 708–711.
- [9] B. Zhao, J. Deng, R. Zhang, L. Liang, B. Fan, Z. Bai, G. Shao and C. B. Park, *Eng. Sci.*, 2018, **3**, 5–40.
- [10] B. Zhao, X. Guo, W. Zhao, J. Deng, B. Fan, G. Shao, Z. Bai and R. Zhang, *Nano Res.*, 2017, **10**, 331–343.
- [11] B. Zhao, X. Zhang, J. Deng, Z. Bai, L. Liang, Y. Li and R. Zhang, *Phys. Chem. Chem. Phys.*, 2018, **20**, 28623–28633.
- [12] B. Belaabed, J. L. Wojkiewicz, S. Lamouri, N. El Kamchi and T. Lasri, *J. Alloys Compd.*, 2012, **527**, 137–144.
- [13] M. Khairy, Synth. Met., 2014, 189, 34–41.
- [14] N. Gandhi, K. Singh, A. Ohlan, D. P. Singh and S. K. Dhawan, *Compos. Sci. Technol.*, 2011, **71**, 1754–1760.
- [15] R. Gangopadhyay and A. De, *Chem. Mater.*, 2000, 12, 608–622.
- [16] F. Qin and C. Brosseau, J. Appl. Phys., 2012, 111.
- [17] M. H. Al-Saleh, W. H. Saadeh and U. Sundararaj, Carbon N. Y., 2013, **60**, 146–156.

- [18] S. Kolev, A. Yanev and I. Nedkov, *Phys. Status Solidi C Conf.*, 2006, **3**, 1308–1315.
- [19] L. Kong, X. Yin, X. Yuan, Y. Zhang, X. Liu, L. Cheng and L. Zhang, *Carbon N. Y.*, 2014, 73, 185–193.
- [20] B. Zhao, J. Deng, L. Liang, C. Zuo, Z. Bai, X. Guo and R. Zhang, *CrystEngComm*, 2017, **19**, 6095–6106.
- [21] B. Zhao, Y. Li, J. Liu, L. Fan, K. Gao, Z. Bai, L. Liang, X. Guo and R. Zhang, *Phys. Chem. Chem. Phys.*, 2018, **20**, 28623 28633.
- [22] Z. Liu, R. Che, Y. Wei, Y. Liu, A. A. Elzatahry, D. Al Dahyan and D. Zhao, *APL Mater.*, DOI:10.1063/1.4979975.
- [23] B. Zhao, J. Liu, X. Guo, W. Zhao, L. Liang, C. Ma and R. Zhang, *Phys. Chem. Chem. Phys.*, 2017, **19**, 9128–9136.
- [24] X. J. Zhang, G. S. Wang, W. Q. Cao, Y. Z. Wei, J. F. Liang, L. Guo and M. S. Cao, *ACS Appl. Mater. Interfaces*, 2014, **6**, 7471–7478.
- [25] M. Han, X. Yin, H. Wu, Z. Hou, C. Song, X. Li, L. Zhang and L. Cheng, *ACS Appl. Mater. Interfaces*, 2016, **8**, 21011–21019.
- [26] R. L. Hadimani, Y. Mudryk, T. E. Prost, V. K. Pecharsky, K. A. Gschneidner and D. C. Jiles, in *Journal of Applied Physics*, 2014, vol. 115.
- [27] S. G. Hunagund, S. M. Harstad, A. A. El-Gendy, S. Gupta, V. K. Pecharsky and R. L. Hadimani, *AIP Adv*.
- [28] R. L. Hadimani, I. C. Nlebedim, Y. Melikhov and D. C. Jiles, *J. Appl. Phys.*, 2013, **113**, 17A935.
- [29] R. L. Hadimani, S. Gupta, S. M. Harstad, V. K. Pecharsky and D. C. Jiles, *IEEE Trans. Magn.*, , DOI:10.1109/TMAG.2015.2446774.
- [30] L. F. Chen, C. K. Ong, C. P. Neo, V. V. Varadan and V. K. Varadan, *Microwave Electronics*, 2004.
- [31] B. Zhao, X. Guo, W. Zhao, J. Deng, G. Shao, B. Fan, Z. Bai and R. Zhang, *ACS Appl. Mater. Interfaces*, 2016, **8**, 28917–28925.
- [32] Zhibo Guo, Hailong Huang, Ding Xie and Hui Xia, Scientific report, 2017, 7: 11331.
- [33] H. Lv, Y. Guo, G. Wu, G. Ji, Y. Zhao and Z. J. Xu, ACS Appl. Mater. Interfaces, 2017, 9, 5660–5668.
- [34] X. Huang, J. Zhang, M. Lai and T. Sang, J. Alloys Compd., 2015, 627, 367–373.
- [35] P. J. Bora, I. Azeem, K. J. Vinoy, P. C. Ramamurthy and G. Madras, *Compos. Part B Eng.*, 2018, **132**, 188–196.
- [36] X. Ni, Z. Zheng, X. Xiao, L. Huang and L. He, *Mater. Chem. Phys.*, 2010, **120**, 206–212.
- [37] C. Guo, F. Xia, Z. Wang, L. Zhang, L. Xi and Y. Zuo, *J. Alloys Compd.*, 2015, **631**, 183–191.
- [38] J. Wang, H. Zhou, J. Zhuang and Q. Liu, Phys. Chem. Chem. Phys., 2015, 17, 3802–12.
- [39] H. Lv, G. Ji, X. Liang, H. Zhang and Y. Du, *J. Mater. Chem. C*, 2015, **3**, 5056–5064.

- [40] M. Wu, H. He, Z. Zhao and X. Yao, J. Phys. D. Appl. Phys., 2000, 33, 2398–2401.
- [41] L. Wang, Y. Huang, X. Ding, P. B. Liu and M. Zong, *Micro Nano Lett.*, 2013, **8**, 391–394.
- [42] G. Sun, X. Zhang, M. Cao, B. Wei and C. Hu, J. Phys. Chem. C, 2009, 113, 6948–6954.
- [43] X. Sun, J. He, G. Li, J. Tang, T. Wang, Y. Guo and H. Xue, *J. Mater. Chem. C*, 2013, **1**, 765–777.
- [44] P. J. Bora, N. Mallik, P. C. Ramamurthy, Kishore and G. Madras, *Compos. Part B Eng.*, 2016, **106**, 224–233.
- [45] D. Micheli, C. Apollo, R. Pastore and M. Marchetti, *Compos. Sci. Technol.*, 2010, **70**, 400–409.
- [46] P. Liu, L. Li, et.al., *Phys. Status Solidi A.*, 2017, **214**, 1700589.
- [42] G. Sun, X. Zhang, M. Cao, B. Wei and C. Hu, J. Phys. Chem. C, 2009, 113, 6948–6954.
- [43] X. Sun, J. He, G. Li, J. Tang, T. Wang, Y. Guo and H. Xue, *J. Mater. Chem. C*, 2013, **1**, 765–777.
- [44] P. J. Bora, N. Mallik, P. C. Ramamurthy, Kishore and G. Madras, *Compos. Part B Eng.*, 2016, **106**, 224–233.
- [45] D. Micheli, C. Apollo, R. Pastore and M. Marchetti, *Compos. Sci. Technol.*, 2010, **70**, 400–409.
- [46] P. Liu, L. Li, et.al., *Phys. Status Solidi A.*, 2017, **214**, 1700589.

Supporting Information

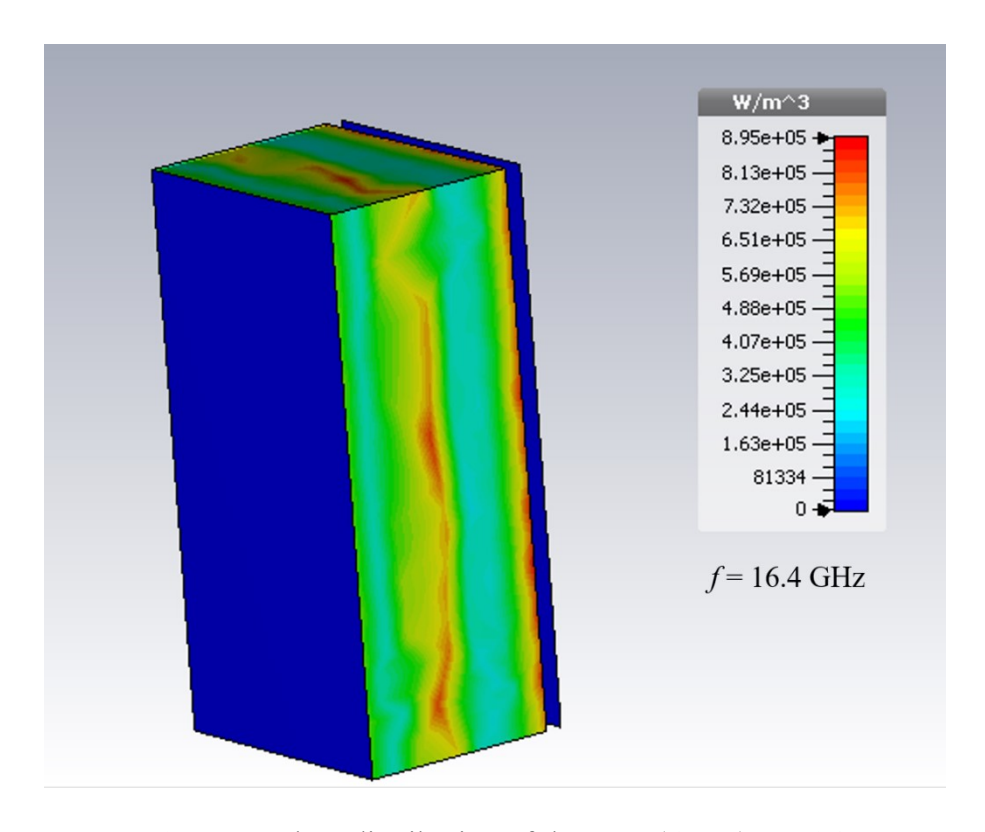


Fig.S1. Power loss distribution of the PGS (6 mm) at 16.4 GHz.

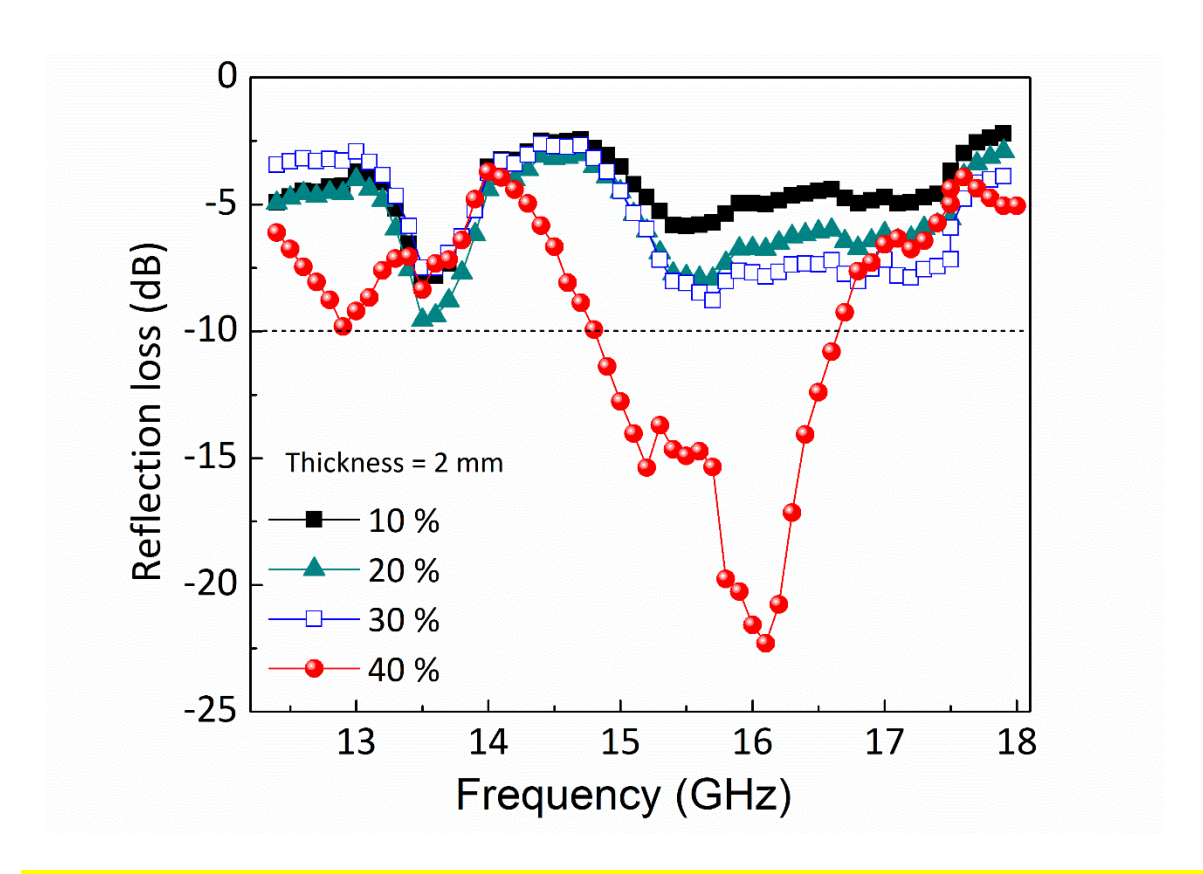


Fig.S2. Ku-band reflection loss (RL) for different loading of Gd₅Si₄ (10 wt.%, 20 wt.%, 30 wt.% and 40 wt.%) nanoparticles in PDMS matrix (thickness 2 mm).